Title

Robust pluripotent stem cell expansion and cardiomyocyte differentiation via geometric patterning

Journal

Integrative Biology, 5(12)

ISSN

1757-9694

Authors

Myers, Frank B
Silver, Jason S
Zhuge, Yan
et al.

Publication Date

2013-12-18

DOI

10.1039/c2ib20191g

Peer reviewed

Published in final edited form as:
Integr Biol (Camb). 2013 December ; 5(12): 1495–1506. doi:10.1039/c2ib20191g.

Robust Pluripotent Stem Cell Expansion and Cardiomyocyte Differentiation via Geometric Patterning

Frank B. Myers[1,2], **Jason S. Silver**[1,2], **Yan Zhuge**[3,4,5], **Ramin E. Beygui**[3,4], **Christopher K. Zarins**[3,4,5], **Luke P. Lee**[1,2,3,4,*], and **Oscar J. Abilez**[5,6,7,8,9,*]

[1]Department of Bioengineering, University of California, Berkeley, CA 94720, USA

[2]Department of Electrical Engineering and Computer Science, University of California, Berkeley, CA 94720, USA

[3]Biophysics Program, University of California, Berkeley, CA 94720, USA

[4]Berkeley Sensor and Actuator Center, University of California, Berkeley, CA 94720, USA

[5]Department of Surgery, Stanford University, Stanford, CA 94305, USA

[6]Cardiovascular Institute, Stanford University, Stanford, CA 94305, USA

[7]Bio-X Program, Stanford University, Stanford, CA 94305, USA

[8]Department of Bioengineering, Stanford University, Stanford, CA 94305, USA

[9]Cardiovascular Medicine, Stanford University, Stanford, CA 94305, USA

Abstract

Geometric factors including the size, shape, density, and spacing of pluripotent stem cell colonies play a significant role in the maintenance of pluripotency and in cell fate determination. These factors are impossible to control using standard tissue culture methods. As such, there can be substantial batch-to-batch variability in cell line maintenance and differentiation yield. Here, we demonstrate a simple, robust technique for pluripotent stem cell expansion and cardiomyocyte differentiation by patterning cell colonies with a silicone stencil. We have observed that patterning human induced pluripotent stem cell (hiPSC) colonies improves the uniformity and repeatability of their size, density, and shape. Uniformity of colony geometry leads to improved homogeneity in the expression of pluripotency markers SSEA4 and Nanog as compared with conventional clump passaging. Patterned cell colonies are capable of undergoing directed differentiation into spontaneously beating cardiomyocyte clusters with improved yield and repeatability over unpatterned cultures seeded either as cell clumps or uniform single cell suspensions. Circular patterns result in a highly repeatable 3D ring-shaped band of cardiomyocytes which electrically couple and lead to propagating contraction waves around the ring. Because of these advantages, geometrically patterning stem cells using stencils may offer greater repeatability from batch-to-batch and person-to-person, an increase in differentiation yield, a faster experimental workflow, and a simpler protocol to communicate and follow. Furthermore, the ability to control where

[*]Corresponding authors: ojabilez@stanford.edulplee@berkeley.edu.

cardiomyocytes arise across a culture well during differentiation could greatly aid the design of electrophysiological assays for drug-screening.

Introduction

The promise of therapeutic tissue engineering and regenerative medicine from stem cells opens a number of exciting engineering opportunities for the cost-effective, safe production of cells for therapy.[1] With the emergence of defined media and feeder-free systems for stem cell maintenance,[2–7] we are moving toward a robust set of techniques which can enable the production of therapeutically-relevant stem cells and their derivatives with industrial scale and quality control. However, pluripotent stem cells are typically maintained and differentiated in 2D monolayer colonies or 3D aggregates ("embryoid bodies") and the geometry of these colonies/aggregates plays a critical role in maintaining pluripotency and enabling successful differentiation into desired cell types.[8–11] Controlling stem cell colony geometry is impossible with conventional cell culture techniques such as clump passaging,[12] and although geometric cell patterning is not a new concept,[13–19] it is not widely employed because existing patterning techniques require tools which are not readily available in a typical biology laboratory. We sought to find a simple, yet powerful solution for patterning stem cells in 2D in order to improve robustness in pluripotency maintenance and differentiation yield.

Much work has focused on the biochemical factors governing cell fate,[20] but geometry and mechanics clearly play a role as well,[21–25] and this role is currently poorly understood. Pluripotent stem cells form isolated colonies, with optimal diameters in the range of 100-2000 μm. Very large colonies tend to form dense, multilayer centers which undergo spontaneous differentiation. Furthermore, when expanding colonies merge together, the dense region between the colonies often results in spontaneous differentiation. On the other hand, very small colonies or individual cells not part of a colony tend to spontaneously differentiate or die.

For many stem cell differentiation protocols, the basic unit of differentiation is not the individual cell, but rather the individual colony, as intra-colony signaling appears to play a role in lineage specification.[25] This is not surprising since during embryonic development, contact-mediated signaling (e.g. Notch/Delta[26]) and paracrine signaling (e.g. Wnt[27] and TGF-β[28]) among neighboring cells play a central role in determining cell fate, a process known as conditional specification. Just as changes in the shape of these signaling gradients can have profound effects on developmental phenotype,[29] the geometry of stem cell colonies plays a significant role in their capacity for pluripotency[11] and differentiation.[22] Cardiovascular disease is an important therapeutic target for stem cell biology, and increasing the yield and subtype of cardiomyocyte differentiation is currently a major goal.[30] It has been previously shown that when differentiated from 3D embryoid bodies (EBs), cardiomyocyte yield depends on EB diameter,[10,31] and several techniques have emerged for generating monodisperse EBs.[32,33] But EB differentiation is difficult to track over time with standard microscopy and provides little insight into the dynamics of cell-cell signaling, maturation, and migration within the EB which facilitate cardiogenesis.

Differentiation from monolayer colonies, on the other hand, allows for easy microscopic observation. For these reasons, we set out to control geometric parameters of monolayer stem cell colonies with the goal of producing cells which were uniformly pluripotent, showed a low incidence of spontaneous differentiation, and improved robustness and yield in cardiomyocyte differentiation.

Our approach is to use an elastomeric stencil to pattern extracellular matrix (Matrigel) and localize pluripotent stem cell colonies onto well-defined circular patterns with diameters in the range of 500-2000 μm. The size, shape, and density of an individual colony can be optimized for a given protocol and is only limited by the resolution of the stencil cutting method. The spacing between neighboring colonies can be tuned to minimize signaling between neighboring colonies and optimize the number of cells per unit area. Stencil patterning has been previously demonstrated,[13,17] however, unlike previous approaches our technique does not require photolithography for stencil fabrication and uses an inexpensive raw material that is readily available in bulk quantities. Stencils can either be cut using simple hand tools or with automated CNC laser, blade, or waterjet cutting tools. Matrigel is a hydrogel that gels at room temperature and must be kept cold during application. During incubation at 37° C, the Matrigel in solution gradually forms a self-assembled thin film on the tissue culture surface. This renders it incompatible with many other protein patterning techniques (stamping, inkjet printing, etc.). It is therefore particularly well-suited for stencil patterning, which places no restrictions on solution temperature and allows long-term incubation of the solution with the surface to be patterned. When used with the commercial and widely-used Matrigel/mTeSR-1 pluripotent stem cell culture system,[7] our stencil patterning technique does not require any modification to the conventional hPSC maintenance protocol. Figure 1 illustrates the importance of geometric control over intra-colony signaling in general (A-B) and for pluripotency specifically (C-E).

Results

Stencil patterning promotes uniform colony size, shape, and cell density

For stem cell maintenance, we designed a 10 × 10 array of 1 mm circular colonies at 2 mm pitch (Figure 1C). This design was based on our own experience with hiPSCs using the mTeSR1/Matrigel system and the manufacturer's recommended protocol[12] which suggests that 150 colonies per well in a 6-well plate are an ideal density for pluripotency (our patterns do not extend over the entire well, so 100 colonies is roughly an equivalent density). We hypothesized that identical colony geometry and cell seeding density would effectively eliminate variability in phenotype arising from microenvironmental heterogeneity. We compared patterned stenciled colonies to unpatterned colonies generated using the mTeSR1 manufacturer recommended clump-passaging technique.

Our stencils are made from a sheet of commercially-available silicone elastomer material and cut using an inexpensive CO_2 laser engraver. If a laser engraver is not available, handheld hole punchers can be used instead. Laser cutting takes less than 2 minutes and stencils can be cleaned and prepared for use in about 5 minutes. Laser cutting has the added advantage that arbitrary patterns can be cut. Silicone stencils reversibly adhere to polystyrene and glass culture surfaces and form a watertight seal via van der Waals forces.

After Matrigel incubation with the stencils, we deposited a single cell suspension of hiPSCs onto stenciled culture surfaces and allowed cells to attach. Stencils were removed after one day. hiPSCs expanded to fill the 1 mm patterns but did not expand beyond these patterns for up to 6 days. Beyond 6 days, cells became overcrowded and began spontaneously differentiating, which sometimes prompted them to expand beyond the patterns (presumably because they began secreting their own ECM). If growth beyond these patterns is desired, Matrigel can be added to the cell culture medium (provided that it is kept cold) and incubated with the cells. This technique is applied during our cardiomyocyte differentiation experiments, described below. Following Matrigel addition, cells migrate beyond their initial pattern boundaries.

We examined the relationship between pluripotency expression and geometric factors including cell density and colony size. We used image analysis to identify colony boundaries from epifluorescence mosaics of DAPI (Figure 2A) and quantified colony area and cell count in these colonies (Figure 2B-C). While colony area was fixed according to the pattern size, cells continue to proliferate within patterned colonies, making cell density a strong function of time (Figure 2D). Cells seeded uniformly across the entire 10 × 10 array, and by varying the single cell suspension concentration, the time-to-confluence and the cell density at a given timepoint can be tuned (see supplementary information). By contrast, unpatterned colonies seeded via conventional clump passaging[12] show a very heterogeneous distribution of cell density and colony size. Furthermore, it is impossible to independently control colony size and cell density using clump passaging.

Uniform cell density improves homogeneity in pluripotency expression

Using stencil patterning, we observed hiPSCs form uniform colonies with morphological and protein expression patterns characteristic of pluripotent cells. Figure 1C shows an epifluorescence mosaic of an entire array of patterned hiPSC colonies. Note that the pluripotency marker SSEA4 is uniformly expressed throughout the array. In unpatterned clump passaged cell colonies (Figure 1B), SSEA4 expression is more heterogeneous and regions that are very dense or very sparse tend to have lower SSEA4 expression.

To quantitatively explore the relationships between cell density, colony geometry, and pluripotency, we used immunofluorescence image analysis to compare the level of the pluripotency transcription factor Nanog to the local cell density, as quantified with a nuclear stain (DAPI). We chose Nanog because it is primarily associated with the nucleus and would therefore colocalize with DAPI; however analysis of SSEA4 signal yielded similar results (see Supplemental Figure 1). In unpatterned cell cultures at D2, D4, and D6, we observed a similar trend in pluripotency vs. local cell density, with a peak at about 12k cells/mm^2 and a relative reduction in pluripotency at higher and lower densities (Figure 3A). This trend agrees with a previous report which used a similar analytical approach to show that pluripotency expression increases with cell density from 0-2.5k cells/mm^2.[8] In that report, only very sparse cells were analyzed, so the downward trend at high density was not observed. Here, we report the first measurement of an optimal density for pluripotency maintenance in 2D colonies (12k cells/mm^2). This result agrees with our previous observations that very sparse and very dense colonies tended to lose pluripotency and

spontaneously differentiate (Figure 1E). The pluripotency vs. density trend among these different timepoints was not substantially different. We performed the same analysis on patterned cells (Figure 3B) and observed that these cells showed a tighter distribution of both density and pluripotency expression and furthermore their pluripotency expression tended to lie along the same pluripotency-density trend line we observed in the unpatterned case. We therefore conclude that cell density is a critical parameter in maintaining pluripotency and that cells patterned into colonies from an enzymatically-generated single cell suspension do not show substantially different pluripotency vs. density characteristics from colonies formed from clump passaging. Finally, we confirm our previous observation that density is a strong function of culture time with patterned colonies, and we see that cells show optimal pluripotency around D2-D4 using our 1 mm patterns and an initial seeding density of 400,000 cells/ml.

We performed a similar analysis on a colony-by-colony basis (Supplemental Figure 3A-B), in which the mean pluripotency and mean cell density were compared. Again, we found a similar inverse relationship between pluripotency and density beyond about 10k cells/mm^2. In contrast with cell density, pluripotency does not seem to be a strong function of colony size (Supplemental Figure 3C-D). Finally, we looked at heterogeneity of pluripotency markers within a colony. We found that larger unpatterned colonies tended to have dense centers which gave rise to spontaneous differentiation and a loss of pluripotency marker expression. Day 4 patterned colonies exhibited uniformly high pluripotency. Figure 3C shows pseudocolored heatmaps generated from the ratio of Nanog immunofluorescence intensity to DAPI intensity and Figure 3D compares a linescan through this heatmap for D4 unpatterned and patterned colonies. Excerpts from the raw fluorescent mosaic images used in this analysis are provided in Supplemental Figure 1.

Flow cytometry indicates that overall SSEA4 expression at day 4 in patterned cultures was equivalent or higher than that of unpatterned cultures (Figure 3E and Supplemental Figure 4). Likewise, quantitative PCR indicated no statistically significant difference in overall gene expression across a panel of 3 pluripotency and 9 early germ-layer differentiation markers (Figure 3F), further indicating that patterning cells from a single cell suspension has no adverse effect on cells as compared with conventional culture techniques.

Patterning improves cardiomyocyte differentiation yield and repeatability

We further examined the capacity for patterned hiPSCs to undergo directed differentiation to the cardiomyocyte lineage. During differentiation, cardiomyocytes generally arise in areas of higher cell density and often form 3D aggregates. We hypothesized that the ability to control local cell density would enable more predictable differentiation. Figure 4A shows time-lapse phase contrast mosaics from three different cell seeding conditions: (1) 2 mm stencil patterns seeded from a single cell suspension, (2) an unpatterned well seeded from a single cell suspension, and (3) conventional scrape passaging producing initial cell clumps of ~500 μm diameter each. After 15 days, all wells were fixed and stained for cTnI and DAPI. Patterned cultures typically lead to a ~4 mm ring of cTnI cells, and this ring is also seen to spontaneously contract (see Videos 1-6). In all cases, cardiomyocytes (as confirmed via cTnI staining and visible contractions) tend to arise in regions of high density which

appear phase-dark and often have three-dimensional structure. This is most evident in the patterned cultures, but the unpatterned cultures also show smaller, punctate regions of higher density which give rise to cardiomyocytes.

Many cardiomyocyte differentiation protocols have been reported in the literature, some of which call for a uniform monolayer of cells and others which call for clump passaging.[34–37] We examined the effect of patterning across six different differentiation conditions (C1-C6) to determine if this technique was broadly applicable or whether it was only useful for certain conditions (e.g. protein growth factors plus small molecules vs. small molecules alone). Figure 4A shows the results of one well from C5, which is one of the few conditions which resulted in successful differentiation across patterned single-cell, unpatterned single-cell, and unpatterned clump techniques. We examined four replicates of each condition (24 total cultures). Patterned cultures from single cell suspensions resulted in spontaneously beating cardiomyocyte regions by day 14 which stained positive for cTnI in 24/24 wells (see Supplemental Figure 5 and Videos 1-6). By contrast, unpatterned cultures seeded from single cell suspensions resulted in 14/24 wells with cardiomyocytes (individual condition results are as follows: C1-2: 0/4, C3: 4/4, C4: 4/4, C5: 3/4, C6: 3/4). Unpatterned cultures seeded from cell clumps resulted in 2/24 wells with cardiomyocytes (C1-C4: 0/4, C5: 1/4, C6: 1/4). In those wells which did not result in cardiomyocytes, cells became overcrowded and completely detached. We used immunofluorescence mosaics to quantify overall yield as the ratio of cTnI+ area to overall cell area (as determined via DAPI). Figure 4B shows that patterned cultures resulted in significantly higher yield in C1-C3 and C6 versus unpatterned single cell cultures and significantly higher yield for all conditions versus clump-passaged cultures. Patterning also results in a predictable cardiomyocyte geometry and location, which would greatly enable screening assays. Figure 4C shows an individual cardiomyocyte generated from a patterned culture. The cell shows sarcomeric banding patterns characteristic of cardiomyocytes.

Figure 5A shows pseudocolored heatmaps indicating the relative expression of cTnI vs. DAPI for multiple replicates of patterned cultures differentiated with each of six different conditions. Note the prominent ~4 mm diameter cardiomyocyte rings which appear in most of the cultures and are especially prominent in C5 and C6. We computed circular linescans to examine the cTnI expression as a function of radius from the center of colony patterns. These linescans are shown in Figure 5B for each differentiation condition. Note that most conditions result in cardiomyocyte enrichment at a ~2 mm radius from the pattern center. C1-C3 result in a more diffuse distribution of cardiomyocytes, but in many cases a second, smaller ring with a radius of ~0.5-1 mm can be observed.

Discussion

We have shown that hiPSCs cultured on stencil patterned substrates exhibit uniform geometry, cell density, morphology, and pluripotency marker expression. Cells seeded with very good uniformity across an entire culture well, with each patterned colony behaving more or less similarly. By varying the initial seeding density, the time-to-confluence and the density at a given timepoint can be tuned. We suggest that cell density, rather than colony size or time in culture, is a critical parameter which must be controlled in order to maintain

pluripotency, and stencil patterning is a scalable approach that provides an easy way to control this parameter across many colonies. We show that cell density is much more tightly distributed in patterned cultures as compared with clump-passaged cultures. This tight density distribution reduces batch-to-batch as well as cell-to-cell variability of pluripotency markers. Maintaining low variability in pluripotency expression will likely be an important aspect of therapeutic cell production and may improve differentiation reliability. Cells continue to proliferate and remain confined to patterned regions after stencils are removed unless additional Matrigel is added (as is done in our differentiation experiments). Although the mTeSR1 protocol recommends clump passaging and cautions that enzymatic cell dissociation leads to a loss of pluripotency, we find that when single cells are seeded onto patterns at high enough density, pluripotency is reliably maintained, even without the use of ROCK inhibitor.[38]

Most importantly, we demonstrate that stencil patterning can help reduce the unpredictability associated with cardiomyocyte differentiation, improving yield and eliminating sensitivity to person-to-person variations on the same protocol. All patterned wells result in successful cardiomyocyte differentiation across six different differentiation conditions. Our conditions represent adaptations of previously well-established protocols that use both growth factors in combination with small molecules (“Keller Protocol”) or small molecules only (“Palecek Protocol”), however, in the present study, we did not specifically use the “Palecek Protocol” as one of our differentiation conditions that has been reported to give upwards of 90% differentiation efficiency. Using this protocol for other ongoing studies, we have also seen upwards of 90% differentiation efficiency using single cell seeding, with cardiomyocytes forming in dispersed sheets (data not shown). It is interesting to note, that in conditions C1-C3, we also saw less distinct rings of cardiomyocytes and more dispersion of cardiomyocytes when using the small molecule IWR-1, a canonical Wnt inhibitor used to induce cardiogenesis at Day 3 similar to the canonical Wnt inhibitors (IWP-2 and IWP-4) used in the “Palecek Protocol”. This suggests that these small molecule Wnt inhibitors may have different mechanisms of actions than the Dkk-1, SB 431542, and Dorsomorphin factors that are used in the “Keller Protocol” also used at Day 3 to induce cardiogenesis. Future work is aimed at elucidating any apparent differences in cardiogenesis when only small molecules are used.

Cardiomyocytes tend to form ring structures with diameters of ~4 mm and under some conditions appear to form two concentric rings with diameters of 2 and 4 mm. Why cells localize to these regions is unclear, but it may be some combination of membrane tension and cytoskeletal signaling at the colony perimeter, local soluble paracrine signaling gradients across the radius of a colony, or contact-mediated signaling. Because stencil patterning leads to predictable differentiation geometries, it could possibly be a useful tool for creating *in vivo* stem cell models of developmental processes. It would also greatly enable electrophysiological studies using, for example, microelectrode arrays positioned under the cardiomyocyte rings. In many cases, contraction waves propagate continuously around the ring, making for straightforward estimates of conduction velocity and other electrophysiological parameters (see supplemental videos, esp. 7).

It is likely that the geometry of these colonies can be further optimized for cardiomyocyte differentiation yield, and we also expect that protocols for other differentiation lineages would benefit for this stencil patterning technique. Although we did not test patterning other matrices such as laminin,[39] vitronectin,[40] or Geltrex, these substances should reasonably be expected to serve as alternatives to Matrigel, depending on user preference. Using a fully-defined substrate would likely further improve repeatability.

Cell colony geometry has been recognized as an important factor in stem cell fate. Our 2D stem cell patterning technique is analogous to techniques that have been developed for producing monodisperse 3D stem cell embryoid bodies such as the AggreWell system.[32] A major advantage of 2D patterning techniques is that they facilitate easy microscopic observations; in our experience the time required to find beating areas is approximately cut in half. Arraying these patterns in large grids allows for many statistical samples of colonies to be analyzed with automated microscopy and image analysis.

Conclusion

We have demonstrated a cell patterning method which does not require specialized equipment and is readily applied to stem cell maintenance and differentiation protocols. Cell patterning in 2D facilitates microscopic observation and reliably localizes the differentiation process, making it potentially a useful tool in stem cell and developmental biology. As stem cell maintenance and differentiation success are critically dependent on the geometry and size of stem cell colonies, this technique is well-poised to improve yield and scalability in therapeutic cell production. From an industrial scalability and quality control standpoint, the spacing between neighboring colonies can be tuned to ensure that each colony behaves identically and independently while maximizing the number of cells that can be cultured per unit area/media volume. In addition, circular patterns lead to connected rings of cardiomyocytes, and this behavior may be desirable for *in vitro* electrophysiological drug screening assays or for tissue engineering applications. Our future work will examine the broader relationship between pluripotent pattern geometry and resulting cardiomyocyte distribution geometry arising from the differentiation process.

Experimental

Stencil Fabrication

Figure 6 illustrates stencil fabrication and usage. Stencils were cut from 0.01” thick sheets of HT-6240 (40 durometer) silicone rubber sheets (Stockwell Elastomerics, Philadelphia, PA). Stencil designs were drawn using AutoCAD (Autodesk, San Rafael, CA) and cut with an automated CO_2 laser engraver (Universal Laser Systems, Scottsdale, AZ). Note that Stockwell Elastomerics also offers custom laser and waterjet cutting services for this material. Furthermore, stencils need not be cut with a laser but can be cut with blade cutters as well. We have also made stencils with handheld hole punchers (Harris Uni-Core histology punchers, Ted Pella, Redding, CA). For stem cell maintenance and expansion experiments, 35 mm stencils (fitting 6-well plates) were made with 1 mm circular holes in a 10 × 10 grid at 2 mm pitch. For cardiomyocyte differentiation experiments, 15 mm stencils (fitting 24-well plates) were made with a single 2 mm circular hole in the center. After

cutting, stencils were sonicated for 1 min in isopropanol, followed by 1 min in DI water. Sonication was carried out in a 500 mL beaker. To allow many stencils to be cleaned at once without sticking to each other, we fabricated a rack of spring loaded clips which hold them in suspension throughout the beaker. The stencils were blown dry with nitrogen. They were then placed into standard polystyrene culture plates and sterilized for 1 hr under UV. A rack of plungers was fabricated to facilitate easy simultaneous alignment of multiple stencils into 6-well and 24-well plates. Each plunger was coated with Parafilm which prevented stencils from sticking to the plunger during insertion into the plates. Stencils reversibly attached to the polystyrene via van der Walls forces and formed a water-tight seal to the surface. Finally, the plates were inspected to make sure that stencils were uniformly attached and there were no air bubbles or debris between the stencil and plate.

If the well contains a stencil with features < 2mm (such as the 10 × 10 array used in our pluripotency experiments), it is necessary to hydrophilize the surface first. Surface tension around the perimeter of the stencil patterns can prevent liquid from reaching the polystyrene surface. In our experiments, we hydrophilized the surface with a brief oxygen plasma treatment by placing the stenciled plates (without lids) in a reactive ion etcher chamber at 60 W, 200 mTorr, for 30 s (Plasma Equipment Technical Services, Livermore, CA). Following plasma treatment, the stencils were quickly wetted with DPBS. The DPBS was subsequently aspirated (patterned regions do not dewet after aspiration), and coated with Matrigel as described below. If oxygen plasma is not available, simply coating the well with 100% ethanol works for wetting the surface. The ethanol can then be exchanged with PBS through several wash cycles. We tried both techniques (plasma-based and non-plasma-based) and saw no apparent difference in cell attachment, morphology or pluripotency.

hiPSC Maintenance

Human induced pluripotent stem cells (hiPSC) (IMR90) line, WiCell, Madison, WI) were maintained in the pluripotent state in 6-well tissue culture plates through daily feeding (2 mL/well) with mTeSR-1 media (StemCell Technologies, Vancouver, Canada) supplemented with 1x penicillin/streptomycin (Invitrogen, #15140-163, Carlsbad, CA). Cells were clump passaged approximately every 4-6 days, at the time when colonies had expanded enough to begin merging with one another. Prior to passaging, new wells were coated with hESC/hiPSC-qualified Matrigel (BD Biosciences, #354277, San Jose, CA) diluted to 12.5 uL/mL in DMEM (Invitrogen, #10569, Carlsbad, CA) and allowed to incubate at 37° C for at least one hour.

Culturing hiPSCs on 10×10 Patterns in 6-well Plates for Maintenance

Cells were grown to 70% confluence in 6-well plates and washed once with DPBS. Stenciled plates were coated with Matrigel following hydrophilization as described above. Cells were enzymatically dissociated with 1 mL/well Accutase (EMD Millipore) at 37° C for 5 minutes and homogenized via gentle trituration. The Accutase was then diluted by adding 2 mL/well of supplemented mTeSR-1. Cells were centrifuged at 300g for 3 min and resuspended in mTeSR-1. For our cell maintenance experiments, cells were seeded at a concentration of 400k cells/mL with 2 mL of cell suspension per well. This concentration was chosen because it led to colony growth similar to that observed with conventional

scrape passaging (i.e. well is ~30% confluent by day 5 and mean colony diameter is ~1mm. Other concentrations may be used and this choice will affect time-to-confluence (see Supplemental Figure 2). Following seeding, the plate was gently shaken 3X, first back-and-forth, then side-to-side, to distribute the cells evenly across all the patterns. Cells were allowed to attach for 10 minutes before the plate was moved. The stencil was removed during feeding the following day. Cells were fed every day with fresh mTeSR-1. The colonies grew to fill the pattern defined by the stencil with very high fidelity. Optionally, Matrigel may be added to the medium (cold) at a later timepoint to allow cells to grow beyond their initial boundaries.

Culturing hiPSCs onto 2 mm Patterns in 24-well Plates for Differentiation

Cells were passaged as a single cell suspension as described above, except ROCK Inhibitor (Y-27632) was included at a concentration of 10 μM in the cell suspension. This prevented dissociation-induced apoptosis with small concentrations of cells. To conserve Matrigel, only a 25 μL droplet of Matrigel solution was applied directly over the 2 mm spot to be patterned. Similarly, only a 25 μL droplet of cell suspension was used (containing approximately 15,000 cells). Note that no plasma treatment or other wetting technique was used here since these patterns are large enough to avoid trapping bubbles. The cells were allowed to attach at 37° C for 30 minutes, 0.5 mL mTeSR-1 was added (the droplet was not aspirated during this process), and the stencil was immediately removed with sterile forceps. At this concentration, 2 mm colonies were generally completely filled in the next day, showing good border integrity and uniform cell density. When colonies were filled in, the cells were fed with cold mTeSR-1 which contained Matrigel (12.5 uL/mL) and immediately placed back in the incubator to minimize cold shock. This was required to allow the colonies to migrate beyond their 2 mm initial boundaries. The differentiation protocol was initiated when the colonies had filled in, typically two days after seeding. We observed successful differentiation on circular patterns from 1 mm to 2.5 mm, but chose 2 mm because it gave slightly more repeatable results.

Culturing Unpatterned hiPSC Monolayers in 24-well Plates for Differentiation

Wells were patterned with Matrigel per the standard maintenance protocol and a single cell suspension of hiPSCs was generated as described above. 15,000 cells were seeded across the entire well (the same number as was used to seed the 2 mm colonies above) in 0.5 mL media and distributed evenly across the plate by shaking back-and-forth, then side-to-side. We control for cell number here, rather than cell density, because seeding the entire well at an equivalent density to the patterns rapidly results in overconfluence and cell death (cells continue to divide for the first several days of the protocol, so the patterns give them room to continue expanding). The differentiation protocol was initiated typically two days after cells were seeded.

Clump Passaging hiPSCs onto Unpatterned Wells

Cells were grown to 70% confluence in 6-well plates. The destination wells (6- or 24-well plate) were coated with Matrigel and then filled with mTeSR-1 (2 mL for 6-well plates, 0.5 mL for 24-well plates). The colonies in the source well were inspected and colonies which looked too dense or too sparse were aspirated. Cells were scraped from the source well using

a Teflon cell lifter (Corning #3008). Since these experiments deal with large cell clumps, care must be taken to use consistent pipette tip sizes and pipetting speeds to achieve consistent results. Following about 5 s of cell scraping, the scraped cell clumps were drawn into a 5 mL serological pipette and deposited in a 15 mL conical vial. The suspension was triturated slowly 4X, yielding clumps approximately 500 μm in diameter. For cell passaging to 6-well plates, 100 μL of the suspension was withdrawn using a 200 μL micropipette and deposited into each destination well. For differentiation in 24-well plates, a 20 μL micropipette, set to 5 μL, was used to withdraw cell clumps from the conical vial. The pipette tip was placed approximately 1 cm from the bottom of the conical vial, the pipette plunger was quickly depressed to cause the heavier, settled clumps to be resuspended, and then the plunger was slowly withdrawn to draw in these clusters. The clumps were deposited in the destination well and inspected under a microscope. For optimal cardiomyocyte differentiation, generally 3-5 clumps of about 500 μm diameter is ideal. Larger clumps tend to overgrow the well and smaller clumps tend to die. Following clump seeding, the plates were placed in the incubator and shaken 3X, first back-and-forth, then side-to-side, to distribute clumps evenly.

hiPSC Cardiomyocyte Differentiation

Our differentiation medium ("Complete RPMI") consisted of RPMI-1640 media supplemented with B27, 1× non-essential amino acids, 1x penicillin/streptomycin, and 0.1 mM β-mercaptoethanol (RPMI-B27). To this medium, various protein growth factors and small molecules were added over a week-long timetable, based largely on and modified from previously described protocols, including the "Keller Protocol,[36,41] the "Mercola Protocol",[35] the "Palecek Protocol",[34] and the "Matrix Sandwich Protocol".[37] Growth factors came from R&D Systems (Minneapolis, MN) and media constituents came from Invitrogen unless otherwise specified. On the first day (D0) of differentiation, 0.5 or 2.5 ng/mL of BMP-4 (#314-BP-010) was added. On the subsequent day (D1), 12.5 μL/mL cold Matrigel, 10 ng/mL BMP4, 5.0 ng/mL Activin-A (#338-AC), and 5 ng/mL bFGF (#233-FB) were added to cold media and the cells were quickly incubated to minimize cold shock. The solution is added cold to prevent the Matrigel from prematurely gelling. This is the so-called "Matrix Sandwich" method.[37] On D3, 37.5 ng/mL Dkk-1 (#5439-DK), 5 uM SB 431542 (#S4317, Sigma, St. Louis, MO), and 0.5 uM Dorsomorphin (#P5499, Sigma, St. Louis, MO) were added; alternatively on D3, 5 or 10 uM IWR-1 (#681669, Calbiochem, La Jolla, CA) was added. On D5, 37.5 ng/mL Dkk-1 was added for some conditions. On D7, 5 ng/mL bFGF was added for some conditions. On D9, fresh Complete RPMI was added (no growth factors) and changed every two days until D15. A table summarizing the six conditions (C1-C6) is provided in Supplemental Figure 6. On patterned plates, cardiomyocytes generally began spontaneously beating on D8. On unpatterned plates, beating was more variable but generally occurred between D8-D12.

Immunocytochemistry

Primary (#AF1997 (anti-Nanog), #MAB1435 (anti-SSEA4), all R&D Systems; #MAB1691 (anti-cTnI), Millipore) and fluorescently conjugated secondary (Invitrogen, Jackson) antibodies were reconstituted in sterile PBS per manufacturer guidelines. Cells were fixed in 4% PFA (in PBS) for 10-15 min, permeabilized with 0.1% Triton X-100 (in PBS) for 10

min, and blocked with normal goat serum (#50-062Z , Invitrogen) for 10 min at RT. In a 35mm well (6-well plate), 500 μL primary antibody solutions for Nanog and SSEA4 (1:10 dilution in goat serum) were allowed to incubate at RT for 1 hr; for 24-well plates, 200 uL primary antibody solution for cTnI (1:500 dilution in goat serum was also allowed to incubate at RT for 1hr. The cells were washed and incubated with 500 μl secondary antibody (6-well plate) or 200uL secondary antibody (24-well plate) for 1 hr at RT (all 1:1000 dilution in goat serum). Cells were then counterstained with a DAPI solution for 10 min (1 mg/ml DAPI + 0.1% Triton X-100 in PBS). All incubations were done on a plate rocker and cells were washed 2X between each step with 0.05% Tween-20 in TBS. Cells were stored in DPBS at 4C prior to imaging.

Quantitative PCR

Cells were enzymatically dissociated with Accutase from multiwell plates and mRNA was isolated using the Invitrogen PureLink Micro-to-Midi Total RNA Purification System according to the manufacturer's instructions. RNA concentration was measured using a Nanodrop ND-2000 spectrophotometer (Thermo Scientific) and 1 μg total RNA was diluted in 20 μL. RT-PCR was carried out using the Applied Biosystems High Capacity RNA-to-cDNA kit according to the manufacturer's instructions. Custom TaqMan (Applied Biosciences) 96-well PCR plates were ordered which included lyophilized primers for genes associated with pluripotency and early differentiation (shown in Fig 6B). The plates included 12 genes of interest (3 pluripotency, 3 endodermal, 3 mesodermal, and 3 ectodermal), 3 endogenous controls (GAPDH, GUSB, HPRT1), and 1 manufacturing control (18S). The associated TaqMan Assay IDs were: 18S = Hs99999901_s1, GAPDH = Hs99999905_m1, HPRT1 = Hs99999909_m1, GUSB = Hs99999908_m1, NANOG = Hs02387400_g1, OCT4 = Hs00742896_s1, SOX2 = Hs00602736_s1, CXCR4 = Hs00607978_s1, FOXA2 = Hs00232764_m1, SOX17 = Hs00751752_s1, BRACHYURY = Hs00610080_m1, GSC = Hs00418279_m1, MESP1 = Hs00251489_m1, MUSASHI1 = Hs00159291_m1, NESTIN = Hs00707120_s1, SOX1 = Hs00534426_s1 (sequences proprietary). Each gene was examined in triplicate for each sample (96/reactions per experiment). The plates were temperature cycled for 40 cycles in a StepOnePlus realtime PCR system and a ΔC_t value was calculated for each gene vs. the mean Ct value of the endogenous controls. Relative Quantification values were calculated as: RQ = 2^(ΔC_t).

Fluorescence Immunostaining Image Analysis (Pluripotency)

Three-color epifluorescence mosaics (16×21 tiles) comprising DAPI, Nanog, and SSEA4 were acquired with a 5X objective using a Zeiss Axiovert microscope and AxioVision (Zeiss Microimaging). These mosaics covered a total area of about 25×25 mm, roughly the size of a 6-well plate well. All subsequent analysis was carried out with custom MATLAB scripts (Mathworks). Images were stitched and linearly blended together into a single TIF image for analysis. The median image intensity was used to estimate the background, which was then subtracted from each channel. Nanog protein expression images were generated from the ratio of protein immunostain intensity to DAPI intensity. These ratio images were used to generate expression heatmaps and scatter plots. To demarcate colonies, the DAPI image was segmented following binary thresholding, erosion (to eliminate debris <1 cell diameter) and dilation (to merge cells closer than 2 cell diameters into the same colony). The resulting

binary image indicated colony geometries, and several statistics were computed based on these geometries including area, cell density, and cell count. To compute cell density, we assume that total integrated DAPI fluorescence should scale linearly with the number of cells within a given area. We measured the total integrated intensity for several isolated nuclei using ImageJ. To obtain a local cell density image, we smoothed the DAPI image with a 12-pixel (~60 um) radius disk convolution kernel, corresponding to roughly 5 cell diameters. The image was then scaled using our estimate of intensity/cells to yield an image where each pixel represents the number of cells within a 60 μm radius. The expression image could then be compared to the cell density image to determine the effects of local cell density on pluripotency expression on a pixel-by-pixel basis. To determine the overall expression of a colony we first identified the contours of the colony as described above, then computed the ratio of total integrated protein intensity to total integrated DAPI intensity, integrating across all the pixels in the colony.

Fluorescence Immunostaining Image Analysis (Cardiomyocyte Differentiation)

All cells were fixed and stained at day 15. Two-color epifluorescence mosaics (DAPI + cTnI-Alexa594) were acquired with a 5X objective as described above (10×14 tiles for one well of a 24-well plate). Images were stitched together and ratiometric cTnI/DAPI images were computed as described above. For overall cTnI expression quantification, both the cTnI image and the DAPI image were binarized (threshold = 1.1 × image median) and the ratio of cTnI+ area to DAPI+ area was computed. cTnI expression in patterned cultures as a function of radius was computed as follows:

$$ex_{cTnI}(r) = \frac{1}{2\pi r}\int_0^{2\pi}\int_r^{r+\Delta r}\frac{cTnI(r,\theta)}{DAPI(r,\theta)}drd\theta$$

where the center of each pattern was individually determined using ImageJ and Δr was set to 2 pixels (52 μm). The resulting cTnI vs. radius profiles were smoothed with a moving average span of 5 pixels (0.130 μm). The average profile across four wells for a given condition, along with the min/max profiles, are reported in Figure 8.

Flow Cytometry

Cells were dissociated with Accutase (hiPSCs) or Trypsin (hiPSC-CMs), centrifuged at 300g for 3 min, and resuspended in 4% paraformaldehyde at RT for 15 min. Cells were then resuspended in PBS prior to staining. Primary (R&D Systems) and secondary (AlexaFluor dyes, Invitrogen) antibodies were successively incubated with the cells in normal goat serum. Primary antibodies were used at 1:10 dilution and secondary antibodies at 1:1000. Both were incubated at 1 hr on ice. Each sample included a corresponding IgG isotype control (#086599, Invitrogen). Cells were counterstained with DAPI. Cells were analyzed on a BD LSR II flow cytometer and data was analyzed with FlowJo software.

Supplementary Material

Refer to Web version on PubMed Central for supplementary material.

Acknowledgments

We would like to thank Paul Lum of the UC Berkeley Biomolecular Nanotechnology Center. Funding for this work was provided by the Siebel Scholars Foundation (FBM, OJA, and LPL), Human Frontier Science Program (LPL), Stanford Advanced Residency Training at Stanford Fellowship (OJA), California Institute for Regenerative Medicine RC1-00151 (CKZ), National Institutes of Health HL089027 (CKZ), National Science Foundation 0735551 (CKZ), and the National Science Defense and Engineering Graduate (NDSEG) Research Fellowship (FBM).

References

1. Kirouac D, Zandstra P. The Systematic Production of Cells for Cell Therapies. Cell Stem Cell. 2008; 3:369–381. [PubMed: 18940729]
2. Chen G, et al. Chemically defined conditions for human iPSC derivation and culture. Nat. Methods. 2011; 8:424–429. [PubMed: 21478862]
3. Chase LG, Firpo MT. Development of serum-free culture systems for human embryonic stem cells. Current Opinion in Chemical Biology. 2007; 11:367–372. [PubMed: 17692558]
4. Akopian V, et al. Comparison of defined culture systems for feeder cell free propagation of human embryonic stem cells. In Vitro Cell. Dev. Biol. Anim. 2010; 46:247–258. [PubMed: 20186512]
5. Chin ACP, Padmanabhan J, Oh SKW, Choo ABH. Defined and serum-free media support undifferentiated human embryonic stem cell growth. Stem Cells Dev. 2010; 19:753–761. [PubMed: 19686051]
6. Xu C, et al. Feeder-free growth of undifferentiated human embryonic stem cells. Nat. Biotechnol. 2001; 19:971–974. [PubMed: 11581665]
7. Ludwig TE, et al. Feeder-independent culture of human embryonic stem cells. Nature Methods. 2006; 3:637–646. [PubMed: 16862139]
8. Peerani R, et al. Niche-mediated control of human embryonic stem cell self-renewal and differentiation. EMBO J. 2007; 26:4744–4755. [PubMed: 17948051]
9. Bauwens CL, et al. Control of Human Embryonic Stem Cell Colony and Aggregate Size Heterogeneity Influences Differentiation Trajectories. STEM CELLS. 2008; 26:2300–2310. [PubMed: 18583540]
10. Hwang Y-S, et al. Microwell-mediated control of embryoid body size regulates embryonic stem cell fate via differential expression of WNT5a and WNT11. Proceedings of the National Academy of Sciences. 2009 doi:10.1073/pnas.0905550106.
11. Saha K, et al. Surface-engineered substrates for improved human pluripotent stem cell culture under fully defined conditions. Proceedings of the National Academy of Sciences. 2011 doi: 10.1073/pnas.1114854108.
12. Maintenance of hPSCs in mTeSR1 and TeSR2. <http://www.stemcell.com/~/media/Technical%20Resources/0/0/0/29106%20MAN%202%202%203.ashx>
13. Folch A, Jo BH, Hurtado O, Beebe DJ, Toner M. Microfabricated elastomeric stencils for micropatterning cell cultures. J. Biomed. Mater. Res. 2000; 52:346–353. [PubMed: 10951374]
14. Kleinfeld D, Kahler K, Hockberger P. Controlled outgrowth of dissociated neurons on patterned substrates. The Journal of Neuroscience. 1988; 8:4098–4120. [PubMed: 3054009]
15. Kane RS, Takayama S, Ostuni E, Ingber DE, Whitesides GM. Patterning proteins and cells using soft lithography. Biomaterials. 1999; 20:2363–2376. [PubMed: 10614942]
16. Roth E, et al. Inkjet printing for high-throughput cell patterning. Biomaterials. 2004; 25:3707–3715. [PubMed: 15020146]
17. Ostuni E, Kane R, Chen CS, Ingber DE, Whitesides GM. Patterning Mammalian Cells Using Elastomeric Membranes. Langmuir. 2000; 16:7811–7819.
18. Huang NF, et al. A matrix micropatterning platform for cell localization and stem cell fate determination. Acta Biomaterialia. 2010; 6:4614–4621. [PubMed: 20601236]
19. Abhyankar VV, Beebe DJ. Spatiotemporal Micropatterning of Cells on Arbitrary Substrates. Analytical Chemistry. 2007; 79:4066–4073. [PubMed: 17465529]

20. Sullivan, S.; Cowan, C.; Eggan, K. Human Embryonic Stem Cells: The Practical Handbook. Wiley; 2007.
21. Tay CY, et al. Micropatterned matrix directs differentiation of human mesenchymal stem cells towards myocardial lineage. Experimental Cell Research. 2010; 316:1159–1168. [PubMed: 20156435]
22. Ruiz SA, Chen CS. Emergence of Patterned Stem Cell Differentiation Within Multicellular Structures. STEM CELLS. 2008; 26:2921–2927. [PubMed: 18703661]
23. Chen CS, Mrksich M, Huang S, Whitesides GM, Ingber DE. Geometric Control of Cell Life and Death. Science. 1997; 276:1425–1428. [PubMed: 9162012]
24. Flaim CJ, Chien S, Bhatia SN. An extracellular matrix microarray for probing cellular differentiation. Nat Meth. 2005; 2:119–125.
25. Nelson CM, et al. Emergent patterns of growth controlled by multicellular form and mechanics. Proceedings of the National Academy of Sciences of the United States of America. 2005; 102:11594–11599. [PubMed: 16049098]
26. Chiba S. Concise Review: Notch Signaling in Stem Cell Systems. STEM CELLS. 2006; 24:2437–2447. [PubMed: 16888285]
27. Aubert J, Dunstan H, Chambers I, Smith A. Functional gene screening in embryonic stem cells implicates Wnt antagonism in neural differentiation. Nat. Biotechnol. 2002; 20:1240–1245. [PubMed: 12447396]
28. Schuldiner M, Yanuka O, Itskovitz-Eldor J, Melton D, Benvenisty N. Effects of eight growth factors on the differentiation of cells derived from human embryonic stem cells RID C-9488-2009. Proc. Natl. Acad. Sci. U. S. A. 2000; 97:11307–11312. [PubMed: 11027332]
29. Nusslein-Volhard C, Frohnhofer H, Lehmann R. Determination of anteroposterior polarity in Drosophila. Science. 1987; 238:1675–1681. [PubMed: 3686007]
30. Laflamme MA, Murry CE. Heart regeneration. Nature. 2011; 473:326–335. [PubMed: 21593865]
31. Sasaki D, et al. Mass preparation of size-controlled mouse embryonic stem cell aggregates and induction of cardiac differentiation by cell patterning method. Biomaterials. 2009; 30:4384–4389. [PubMed: 19487020]
32. Stover, AE.; Schwartz, PH. Human Pluripotent Stem Cells. Schwartz, PH.; Wesselschmidt, RL., editors. Vol. 767. Humana Press; 2011. p. 391-398.
33. Burridge PW, et al. A Universal System for Highly Efficient Cardiac Differentiation of Human Induced Pluripotent Stem Cells That Eliminates Interline Variability. PLoS ONE. 2011; 6:e18293. [PubMed: 21494607]
34. Lian X, et al. Robust cardiomyocyte differentiation from human pluripotent stem cells via temporal modulation of canonical Wnt signaling. PNAS. 2012 doi:10.1073/pnas.1200250109.
35. Willems E, et al. Small-molecule inhibitors of the Wnt pathway potently promote cardiomyocytes from human embryonic stem cell-derived mesoderm. Circ. Res. 2011; 109:360–364. [PubMed: 21737789]
36. Yang L, et al. Human cardiovascular progenitor cells develop from a KDR+ embryonic-stem-cell-derived population. Nature. 2008; 453:524–528. [PubMed: 18432194]
37. Zhang J, et al. Extracellular matrix promotes highly efficient cardiac differentiation of human pluripotent stem cells: the matrix sandwich method. Circ. Res. 2012; 111:1125–1136. [PubMed: 22912385]
38. Watanabe K, et al. A ROCK inhibitor permits survival of dissociated human embryonic stem cells. Nature Biotechnology. 2007; 25:681–686.
39. Rodin S, et al. Long-term self-renewal of human pluripotent stem cells on human recombinant laminin-511. Nature Biotechnology. 2010; 28:611–615.
40. Prowse ABJ, et al. Long term culture of human embryonic stem cells on recombinant vitronectin in ascorbate free media. Biomaterials. 2010; 31:8281–8288. [PubMed: 20674971]
41. Kattman SJ, et al. Stage-Specific Optimization of Activin/Nodal and BMP Signaling Promotes Cardiac Differentiation of Mouse and Human Pluripotent Stem Cell Lines. Cell Stem Cell. 2011; 8:228–240. [PubMed: 21295278]

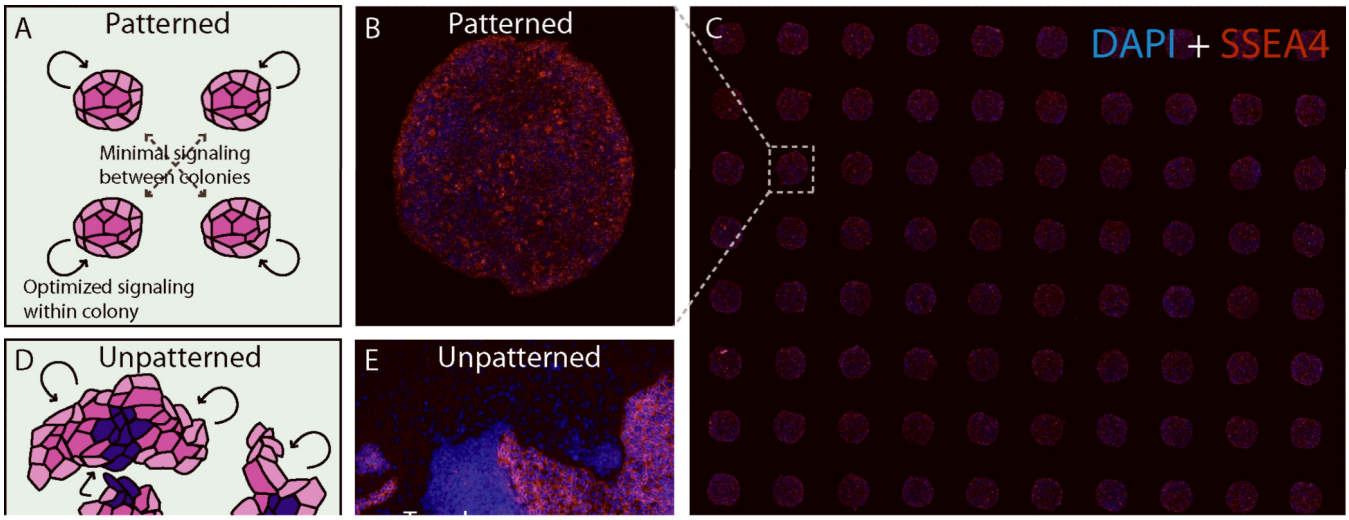

Figure 1.

(A, D) Cell colony geometry impacts paracrine and cell-contact signaling mechanisms, both of which are important for stem cell maintenance and differentiation. Geometric patterning can ensure each colony experiences similar stimulus conditions. A circular geometry ensures there is, at most, a radial dependence on these conditions. Unpatterned stem cell colonies show great heterogeneity as colonies grow asymmetrically and collide, making controlled experimentation and process scale-up difficult. (B-C) Stencil patterning leads to uniform pluripotency of iPSCs, as measured with SSEA4 expression, across all colonies within a culture. (E) Using conventional clump passaging, cells which are very dense or very sparse tend to lose pluripotency.

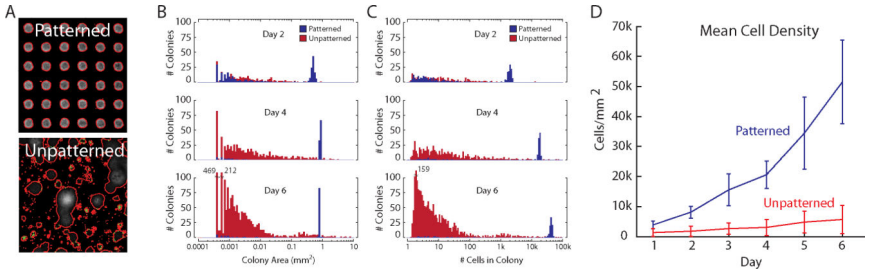

Figure 2.

Stencil patterning allows precise control over colony area and density. (A) Colonies were segmented from DAPI fluorescence microscopy mosaics (See Supplemental Figure 1 for raw images). Colony boundaries were identified (red). (B-C) Colony area and cell count are exponentially distributed in unpatterned cultures (red) but are tightly regulated in patterned cultures (blue) based on the stencil shape. As cells proliferate over time, the colony size remains fixed while cell count increases. (D) Because of patterned cell confinement, cell density is a strong function of culture time.

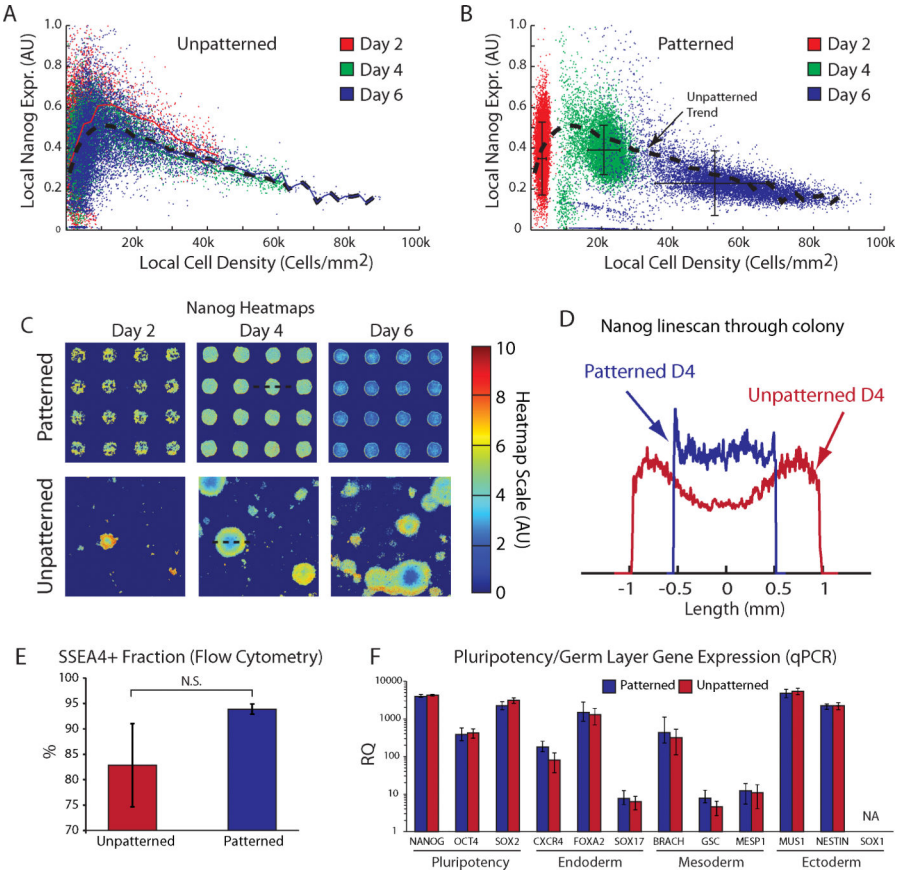

Figure 3.

hiPSC cell density influences pluripotency. Consequently, patterned colonies exhibit more uniform pluripotency. (A) Nanog expression is a function of local cell density in both unpatterned and patterned colonies. Red, blue, and green lines indicate the mean expression vs. density for day 2, 4, and 6, respectively. In all cases, there is an optimal density of about 12k cells/mm^2, where pluripotency is maximized. The substantial overlap among the timepoints indicates that density, rather than time, is the causative parameter. Black dashed line indicates the pooled trend for all days. (B) Patterning shows much more tightly distributed Nanog expression, with an optimal culture time of 2-4 days. Black dashed line indicates pooled trend from (A). (C) Pseudocolored heatmaps comparing Nanog expression in patterned and unpatterned colonies. Note the uniformity in patterned colonies and the nonuniformity in larger unpatterned colonies. This is further illustrated in the linescans in (D), where the black dotted lines in (C, Day 4) indicate from where the linescans are being drawn. (D) Flow cytometry from cells at day 4 indicates that SSEA4 expression in patterned colonies is not statistically significantly different (N.S.) than in unpatterned colonies (n=3 different passages), which is consistent with our microscopy data. Examples of flow cytometry histograms are given in Supplemental Figure 4. (E) A survey of pluripotency and early germ layer differentiation markers reveals that bulk expression is equivalent between patterned and unpatterned colonies, as is the batch-to-batch variability (error bars signify standard deviation among n=3 different passages).

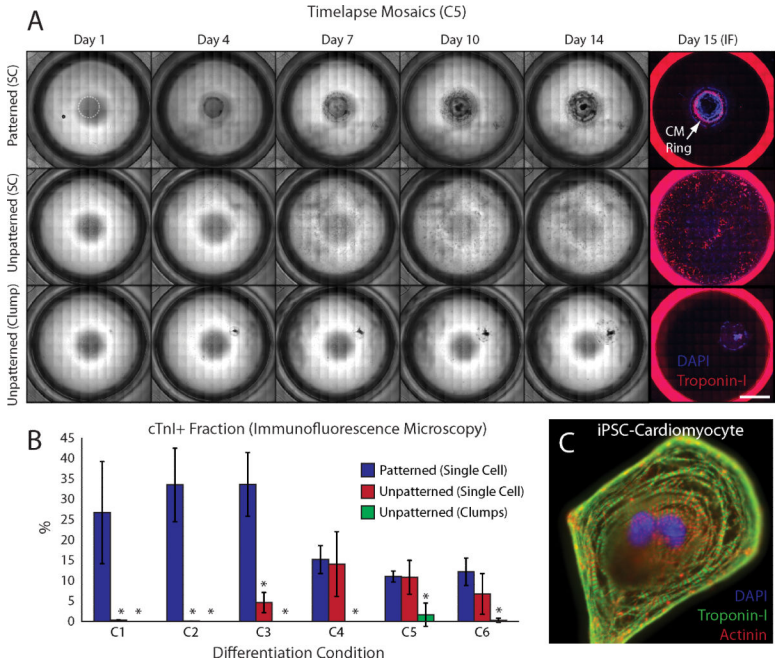

Figure 4.

Patterning improves yield, robustness, and geometric control of cardiomyocyte differentiation. (A) Phase contrast mosaics across individual wells show the evolution of dense cell regions which give rise to cardiomyocytes. White ring at day 1 indicates boundary of initial pattern. These images were taken from differentiation condition C5. Colonies grow somewhat beyond their original 2 mm patterns. Patterned colonies lead to a characteristi ~4 mm diameter ring-shaped region of cardiomyocytes as identified by cardiac Troponin-I (cTnI) at Day 15. Unpatterned cells seeded from a single cell suspension at the same density fail to produce large multicellular structures and result in random pockets of differentiation across the well. Likewise, unpatterned clump-passaged cells do not provide any control of the size or location of a colony. Only one well of four wells of the clump-passaged cells resulted in cTnI+ cells for this condition. Scale bar is 4 mm. (B) Yield is calculated as the fraction of total cell area across a well (as determined by DAPI) where cTnI is expressed (as defined as 10% over the median fluorescence intensity). Error bars indicate standard deviation across four different replicates. Six different differentiation conditions were evaluated (C1-C6). For all conditions, patterning resulted in cTnI+ yields equivalent to or greater than those observed in unpatterned cultures. Yield was significantly higher for patterned cultures in all conditions relative to clump-passaged cultures as well as uniform single cell cultures in C1-C3, and C6. (C) Differentiated cardiomyocytes display characteristic sarcomeric banding with cTnI and actinin. *$p<0.05$

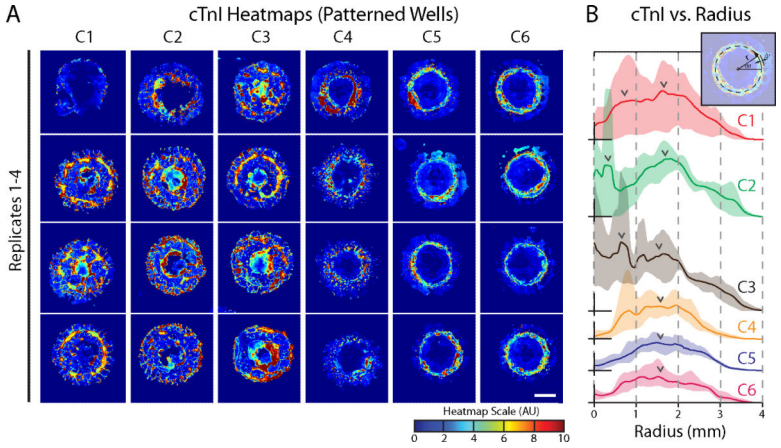

Figure 5.

Cardiomyocyte ring morphology varies somewhat from condition to condition, but is consistent within a given condition. (A) Pseudocolored cTnI expression heatmaps were generated by taking the ratio of cTnI intensity to DAPI intensity on a pixel-by-pixel basis. A ~4 mm cardiomyocyte ring is clearly seen in all differentiation conditions and is particularly prominent in C5 and C6. Conditions C1-C3 tended to yield two concentric rings, with the interior ring at roughly the edge of the original colony (2 mm diameter). Scale bar is 2 mm. (B) The mean cTnI expression across four patterns was plotted as a function of radius from the pattern center. Shaded regions indicate the range between the minimum and maximum expression profiles. Arrows indicate peaks in expression. Note that all conditions result in a local maximum of cTnI expression at ~1.5-2 mm radius. C1-C3 also show a local maximum closer to the original colony edge (~0.5-1 mm). Inset shows radial expression calculation method (see methods).

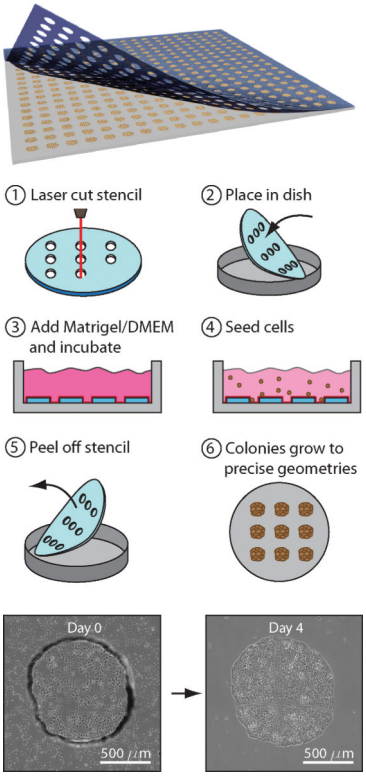

Figure 6.

(Top) Stencils patterning is a scalable approach for generating uniform stem cell colonies across arbitrarily large 2D substrates. (Middle) Overview of stencil patterning technique. Stencils are cut using an automated 2-axis CO_2 laser engraver and cleaned using IPA/water. Stencils are then placed in standard tissue culture polystyrene (TCPS) culture dishes, Matrigel is added per manufacturer instructions, and hiPSCs are seeded in the well from a single cell suspension. (Bottom) Comparison between cells immediately after seeding (with stencil still attached) and resulting filled-in colony at day 4. After cells have attached, the stencil is removed and colonies grow to fill patterns.